

**Energy and Angular Distributions of Secondary Electrons Under High
Electric Field**

Christopher Forbes

Energy and Angular Distributions of Secondary Electrons under High Electric Field

Christopher Forbes

Eastridge Senior High School

LLE Advisor: Paul Jaanimagi

X-ray bombardment of a photocathode produces high-energy primary photoelectrons, which in turn produce a multitude of low-energy secondary electrons. We use a 60° cylindrical analyzer to disperse the secondary electrons onto a phosphor screen, according to their transverse velocity and axial energy. The phosphorescence is recorded with a scientific-grade CCD camera. Changing the electron dispersion allows for full analysis of the energy distribution, particularly the axial component. Under a high-voltage accelerating field, we expect the electron angular and energy distributions to vary from results obtained under a low electric field. The angular distribution ought to become more forward directed than Lambertian, with the energy distribution increasing in the axial direction. We have verified that the transverse energy distribution is not modified by a large axial accelerating field.

I: Introduction

We investigated how a large axial electric field modifies the energy and angular distribution of the secondary electron emission from an x-ray sensitive photocathode. While interest in this topic has existed for over 30 years, no one has ever experimentally measured it. Many scientists have speculated that the angular distribution of the electrons

would not be Lambertian, as it is under low electric field, but that the angular distribution will become more forward directed.¹ Energy is expected to increase in the axial direction, with the transverse energy remaining the same as under low field. Despite all this speculation, no one has ever conducted such an experiment, so these expectations have not been corroborated.

Past experiments have had some similarities to our current research. However, either the electric field was significantly weaker or the distributions were not measured. In an experiment measuring the angular distribution of photoelectrons, it was found to be roughly Lambertian. However, this occurred in a low electric field, which would have minimal impact on the electron distribution.² Henke et al.³ in 1979 published his work on the total energy distribution curves of x-ray induced secondary electron emissions. This experiment did not measure the axial and transverse energy distributions, but only the total energy distribution. Assuming a Lambertian angular distribution, the axial and transverse energy distributions can be calculated using Henke's data (see Figure 1). In a Lambertian angular distribution, the radial energy component is equivalent to the axial energy component. A further past experiment looked at the effect of high electric fields on photocathodes. This found that stronger electric fields resulted in greater electron emissions from photocathodes.⁴ While the experiment was under high field, neither energy nor angular distributions were measured. Despite sharing some similarities, all of these experiments are notably different than our current research.

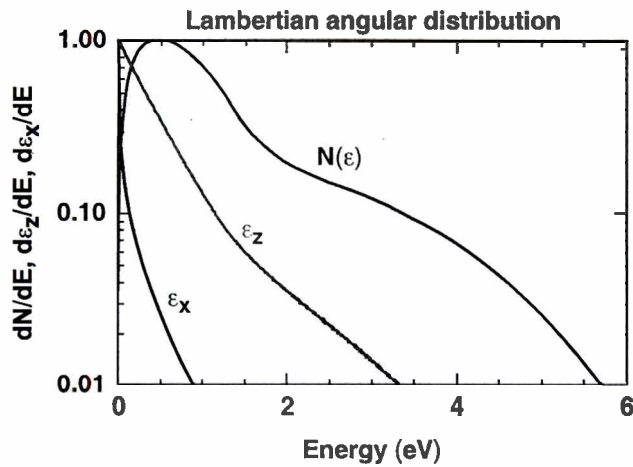


Figure 1: Henke's³ energy distribution curves for a KBr photocathode, assuming a Lambertian distribution. $N(\epsilon)$ is the total energy, ϵ_z is the axial energy, and ϵ_x is a transverse energy component.

Our experiment is designed to measure the axial and transverse energy distributions under a high axial electric field. By measuring the energy distributions, the angular distribution can then be derived. The accelerating electric field reached as high as 12 kV over 4 mm, or 3 kV/mm. A cylindrical analyzer disperses the electrons with either high or low electron dispersion. The dual dispersion modes allow us to determine the axial and transverse energy components. In particular, the axial energy would be difficult to determine if the distribution were non-Lambertian. Even with both high and low dispersion, the axial energy is still challenging to determine. In fact, this experiment has not been conducted previously due to difficulties in measuring the distributions properly. However, through utilization of the cylindrical analyzer, measuring the distributions has become theoretically possible.

This research is significant for a number of reasons. For streak cameras, the time resolution is given by $\Delta t \propto \epsilon_z^{1/2} / E_z$, where ϵ_z is the axial energy and E_z is the axial electric field. By increasing the axial accelerating electric field, time resolution

improves. However, this could also increase the axial energy, worsening the time resolution. Therefore, knowing the effects on the axial energy are essential for improving time-of-flight dispersion for photocathode-based electron sources. Large accelerating fields also allow for increasing the space-charge limited current density, given by $J \propto E_z^{3/2}/d^{1/2}$, where d is the field distance. This means that a stronger field results in a stronger current and consequently, a stronger signal. Our research seeks to experimentally measure the secondary electron distributions under a high accelerating field, as well as to confirm Henke's data taken under a low electric field. This will end speculation and allow for practical use of this knowledge.

In section II, we discuss the background information relevant to understanding our experiment. In section III, the setup used will be presented in detail. Section IV will discuss our experimental results using the cylindrical analyzer.

II: Background

The angular distribution of photoelectrons under low electric field has been previously found to be Lambertian.² Lambert's Law states that the emission in a direction θ is given by $I_\theta = (I_0/\pi)\Delta A \cos \theta$, where ΔA equals the area emitting radiation, and I_0 is the rate of emission per unit area integrated over all angles. A Lambertian distribution is azimuthally symmetric. The radiation emitted in a zone having apex angle θ is $i_\theta = \int_0^\theta di_\theta = I_0\Delta A \sin^2 \theta$.

A photocathode is a material that emits electrons when bombarded with photons of sufficient energy. The energy must be higher than the work function of the material. Any energy the photons have beyond the work function can be transferred to electrons in the form of kinetic energy. A single photon can also produce multiple electrons, or the absorption of multiple photons can release one electron, providing energy levels are appropriate. Most of these emitted electrons are pulled back to the cathode due to electrostatic attraction. However, by using an accelerating electrical field, most of the electrons will escape the attraction of the photocathode.

With x-ray photocathodes, secondary electrons are the principal emission rather than primary photoelectrons (see Figure 2). The primary photoelectrons are high energy and collide with multiple other electrons, giving these secondary electrons the necessary energy for ionization and subsequent release from the photocathode. The secondary

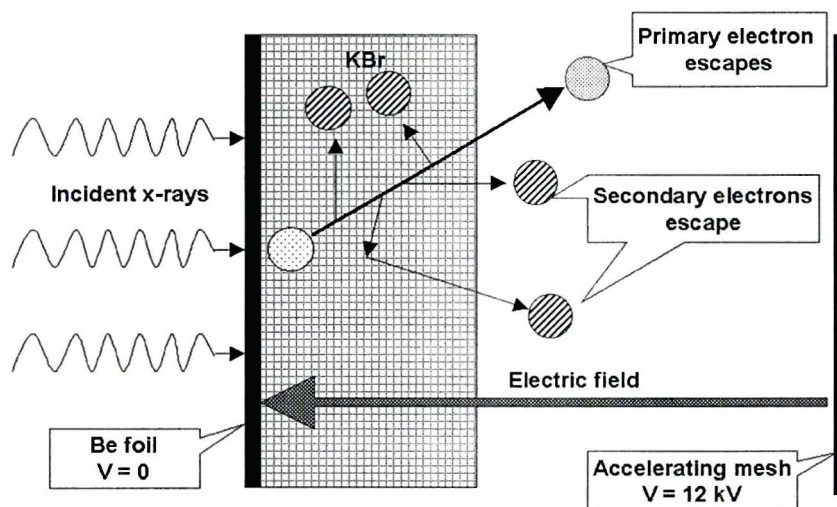


Figure 2: Illustrated is the escape of a high-energy primary electron from a dielectric photocathode. In the escape process, numerous low-energy secondary electrons are produced. A high electric field increases the electron yield from the photocathode.

electrons produced in this manner may outnumber the primaries by a factor of 10 or even 100. While primary electrons are still emitted, for our experiment they amount only to noise. They have too much energy to be directed easily, which is why secondary electrons are used in their stead.

III: Apparatus

The cylindrical analyzer is constructed of aluminum with macor (machinable ceramic) for insulation between metal parts of differing potential. The x rays are produced by a large area x-ray source. This means that illumination is fairly uniform along the photocathode. The entire apparatus is contained within a Ten-Inch Manipulator (TIM), a vacuum chamber with pressures as low as 10^{-8} torr. In practice, the experiment was conducted on the 10^{-7} to 10^{-6} torr range. As such, all of the screws are vented to prevent the gradual leak of air trapped below the screws and in their threads. Furthermore, all the parts are extremely clean to prevent oils from evaporating in the low pressure, as this would increase the pressure within the vacuum chamber. The o-rings must be particularly clean also, as even specks of dust could interfere with establishing a truly airtight seal.

The x rays arriving at the cylindrical analyzer are absorbed in a KBr photocathode. The KBr is coated on a thin layer of beryllium, which supports the coating and carries the photocathode voltage. Half of the beryllium is blocked and has no coating, allowing us to differentiate the signal from the noise. The secondary electron

emissions from this photocathode first travel to the accelerating mesh screen. The photocathode is set at -12 kV and the accelerating mesh can be set at approximately -11.9 kV, -11.59 kV, -8.38 kV, -5.3 kV, and 0 V. This results in an accelerating electrical field at 100 V, 410 V, 3.62 kV, 6.7 kV, and 12 kV over 4 mm, respectively. The mesh screens are made of extremely fine copper and allow for independent variation of electrical fields. Electrons are able to pass through, but electric fields are prevented from spreading to undesired locations.

Next the electrons travel between the accelerating mesh screen and the initial center potential mesh screen. Upon passing through this second screen, the electrons enter the cylindrical analyzer. In the analyzer, electrons travel between concentric cylinders through a 60° arc before encountering another mesh screen. Inside the arc, the

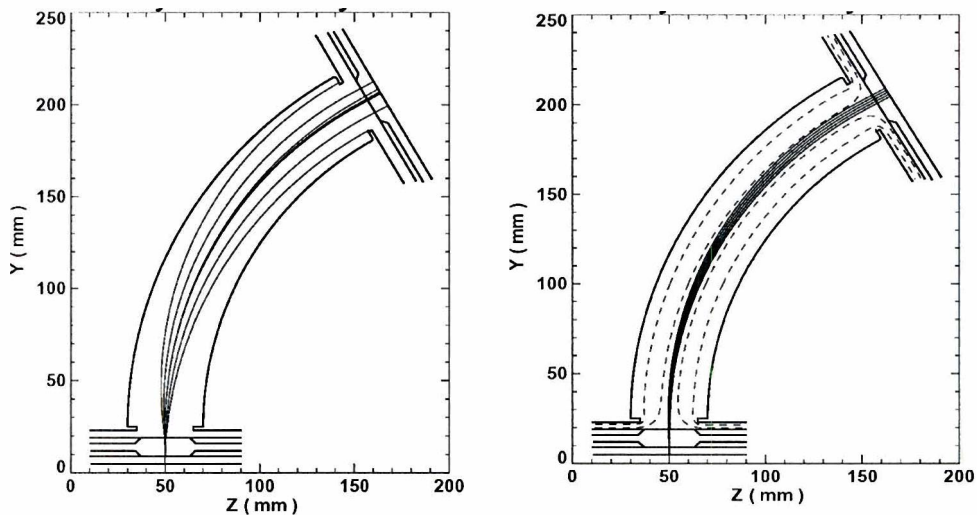


Figure 3: To the left is the electron ray trace of the cylindrical analyzer under high dispersion, and to the right is the ray trace under low dispersion. The dashed lines in the low dispersion image are equipotential lines on 1 kV intervals. The transverse energy of the electrons is dispersed far from the center under high dispersion, with the axial energy dispersed closely around the center. The electron beams originate at the photocathode and terminate at the phosphor screen.

electric field can be adjusted to high or low voltage to control dispersion of the electrons (see Figure 3). The higher voltages, around +2 kV inner and -2 kV outer with center at ground, result in low electron dispersion. High dispersion of the electron distribution is obtained with low voltage on the analyzer (-11.59 kV center).

After passing through the third mesh screen (also center potential), the electrons collide with an aluminized phosphor screen, lighting up wherever they hit. The more electrons that hit a spot, the brighter the phosphor glows. The aluminum coating provides a ground plane, prevents light from entering through the analyzer, and ensures that all light emitted from the phosphor is received by the CCD camera. This collected image can later be analyzed to determine the desired energy and angular distributions.

A Spectral Instruments 800 series CCD camera records the image of the phosphor screen. The CCD is operated at -40° Celsius, chilled by a thermoelectric cooler. This ensures that dark current is kept to a minimum. The camera has a resolution of 2,048 by 2,048, with 13.5 micron pixel size. Exposures were taken for ten second intervals to achieve a large signal to noise ratio. Background was also subtracted from the images for cleaner results.

A 60° arc is used for the cylindrical analyzer due to the source demagnification at that point. This allows us to use a larger electron source, thereby getting a stronger signal. Under low dispersion, the source magnification was 0.1, and under high dispersion it was only 0.03. At 60° the electrons are also well dispersed, with the

analyzer fitting nicely within the vacuum chamber. A larger arc could be difficult to employ for use within the limited space of the vacuum chamber, especially because we need an x-ray source facing the photocathode.

IV: Experimental Results

The most significant finding is the transverse energy distribution. The transverse energy under high electric fields agreed with Henke's data for the total energy distribution and a Lambertian angular distribution (see Figure 4). At low electron energies, the correlation was very strong. However, on reaching higher energy levels, a slight discrepancy developed. While seemingly erroneous, this divergence was consistent with the signal-induced noise we encountered.

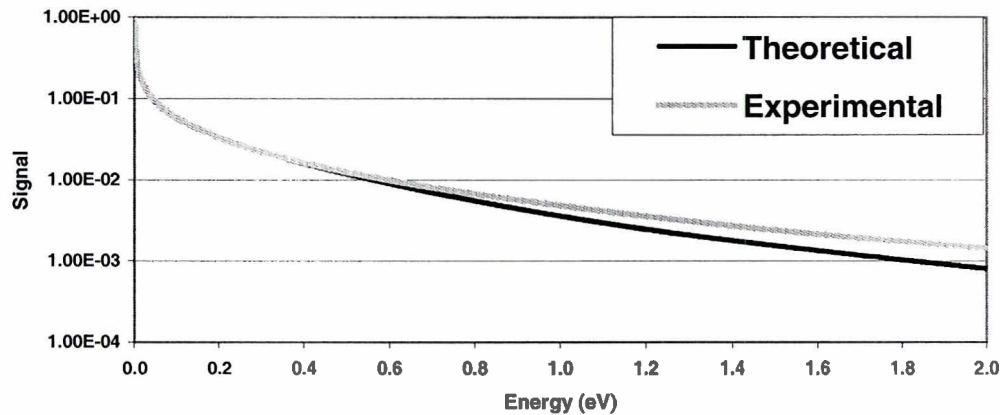


Figure 4: Graph of transverse energy distribution based on Henke's data (Theoretical) versus the transverse energy distribution we measured (Experimental). Note the close correlation at low energy levels, where there was a strong signal. Our data was taken under a 6.7 kV/4 mm electric field in low dispersion mode.

We encountered a significant amount of signal-induced noise. We believe this to be caused by electrons intercepted by the two foremost meshes. We have determined that the noise is from electrons originating by the photocathode end, as the noise shifts with the signal. Electrons produced at the phosphor screen end of the analyzer would not shift when we adjust voltages on the cylinders. The large amounts of signal-induced noise led to distributions leveling off prematurely, giving us increased readings at higher electron energy levels. We also encountered some unexpected asymmetries in some of our images. However, upon analysis there was strong enough signal that the transverse distribution could be derived.

The condition of the photocathode used may have introduced small amounts of error into our data. The photocathode coating was old, and it was visibly apparent that it was not in the best of shape. It had limited exposure to atmospheric conditions, meaning that some moisture was absorbed. This is known to lower the quantum efficiency of photocathodes. However, it is not known whether moisture absorbed by a photocathode modifies the electron angular and energy distributions.

Our data was optimal under a 1.675 kV/mm electric field (see Figure 5). At our highest field (3 kV/mm), the signal-to-noise ratio was worse, resulting in less clean results. The 1.675 kV/mm case had a strong signal, being second highest in voltage, but lacked the level of noise in the 3 kV/mm images. Despite significant noise, we were still able to obtain data at all five voltages under low dispersion. In high dispersion mode, large amounts of signal-induced noise contaminated the broader signal peaks and prevented us from deriving the axial energy distribution.

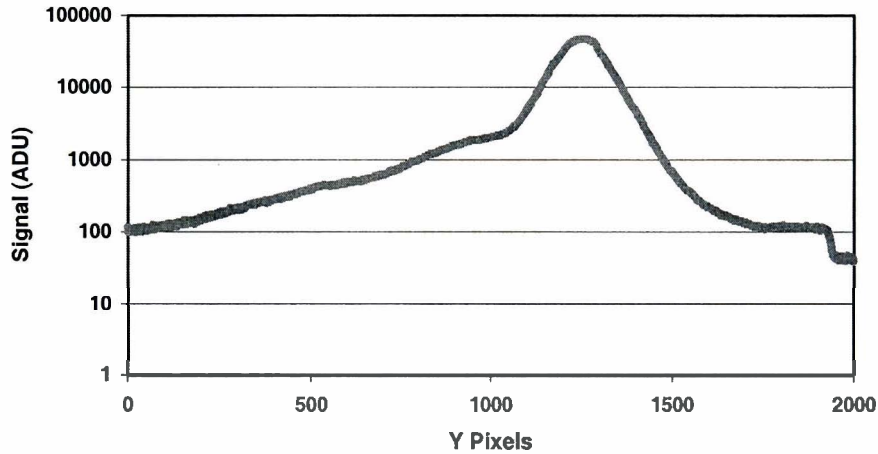


Figure 5: Lineout of image taken in low dispersion mode under a 6.7 kV/4 mm electric field. The transverse velocity is dispersed over space. Visible is the strong signal peak, as well as the signal-induced noise to either side of it.

Obtaining the axial energy distribution relies upon our ability to take clean data under both high and low dispersion. Low dispersion mode isolates the transverse velocity distribution by keeping the axial dispersion under 1 pixel/eV, with the transverse dispersion at $98.5 \text{ pixels}/\sqrt{eV}$. The dispersions are measured from the peak of the signal. Under high dispersion, the transverse dispersion is $558.5 \text{ pixels}/\sqrt{eV}$, while the axial is 20 pixels/eV. By subtracting the transverse energy distribution acquired under low dispersion from the total energy distribution, the axial energy distribution can be found. With both the axial and transverse energy distribution curves, the angular distribution can then be derived.

V: Conclusion

We have verified the transverse energy distribution curves based on Henke's data for the total energy distribution and a Lambertian angular distribution. We also

confirmed that the transverse energy distribution does not change under a high axial accelerating field. Notable levels of signal-induced noise generated by electrons intercepted by the meshes prevented us from extracting the axial energy distribution. Accordingly, the angular distribution under high electric field has not yet been verified.

Future versions of the cylindrical analyzer will be based upon a pulsed system. This should allow for higher accelerating fields, as well as reducing the signal-induced noise. If successful, the axial energy distribution can then be determined. Also, a further look into the copper meshes and any possible substitutes should be taken in an effort to reduce the noise we experienced.

Acknowledgements

First and foremost I would like to recognize my advisor at LLE, Dr. Paul A. Jaanimagi, whose hard work made this project a reality. I would also like to thank Mr. Bob Boni for his assistance in the construction of the setup, and Dr. Stephen Craxton for heading the Summer High School Research Program. Lastly, I would like to express my gratitude for all of the others at LLE who assisted throughout the course of the project. I am truly appreciative of the effort that was put into my project and the summer program as a whole.

References

-
1. J. Cazaux, "A new analytical approach for the transport and the emission yield of secondary electrons from insulators," *Nucl. Instr. and Meth. In Phys. Res. B* **192**, 381-392 (2002).
 2. H.E. Ives, A.R. Olpin, and A.L. Johnsrud, "The distribution in direction of photoelectrons from alkali metal surfaces," *Phys. Rev.* **32**, 57-81 (1928).
 3. B.L. Henke, J. Liesegang, and S.D. Smith, "Soft -x-ray-induced secondary-electron emission from semiconductors and insulators: Models and measurements," *Phys. Rev B, Codens. Matter* **19**(6), 3004-3021 (1979).
 4. J.A. Cochrane and R.F. Thumwood, "The effects of high electric fields on photocathodes," *Advances in Electronics and Electron Physics* **40A**, 441-449 (1976).